A Compliant and Creep Resistant SAC-Al(Ni) Alloy

By

Dr. Benlih Huang, Dr. Hong-Sik Hwang, and Dr. Ning-Cheng Lee
Indium Corporation of America
Clinton, NY
Tel: (315) 853-4900, Fax: (315) 853-1000, Email: askus@indium.com

ABSTRACT

Addition of Al into SAC alloys reduces the number of hard Ag_3Sn and Cu_6Sn_5 IMC particles, and forms larger, softer non-stoichiometric AlAg and AlCu particles. This results in a significant reduction in yield strength, and also causes some moderate increase in creep rate. For high Ag SAC alloys, adding Al 0.1-0.6% to SAC alloys is most effective in softening, and brings the yield strength down to the level of SAC105 and SAC1505, while the creep rate is still maintained at SAC305 level. Addition of Ni results in formation of large $(Ni,Cu)_3Sn_4$ IMC particles and loss of Cu_6Sn_5 particles. This also causes softening of SAC alloys, although to a less extent than that of Al addition. Addition of Al also drives the microstructure to shift from near-ternary SnAgCu eutectic toward combination of eutectic SnAg and eutectic SnCu. Addition of Ni drives shifting toward eutectic SnAg. For SAC+Al+Ni alloys, the pasty range and liquidus temperature are about 4°C less than that of SAC105 or SAC1505 if the addition quantity is less than about 0.6%. Addition of Al and Ni also results in a slight decrease in modulus and elongation at break, although the tensile strength is not affected.

Key Words: solder, lead-free, SAC, soften, compliant, creep resistant, Al, Ni

I. INTRODUCTION

The Sn-Ag-Cu (SAC) alloys have been considered promising replacements for the lead-containing solders for the microelectronics applications. However, due to the rigidity of the SAC alloys, compared with the Pb-containing alloys, more failures have been found in the drop and high impact applications for the portable electronic devices, such as the personal data assistant (PDA), cellular phone, notebook computer..etc.

Reducing the Ag concentration of the SAC alloy has been shown to result in a more ductile and compliant solder for the high impact conditions [1]. However, in comparison with the high Ag, Ag ≥ 3%, containing SAC alloys, (e.g. SAC305, SAC405, etc.), these lower Ag-containing SAC alloys, Ag ≤ 2%, (e.g., SAC205, SAC105… etc.), exhibit poorer creep and thermal fatigue performance thus are limited in their potential applications in the electronic industries. In addition, the pasty range of these low Ag containing SAC alloys increased with decreasing Ag content therefore they may result in higher defect rates in reflow for these low Ag containing SAC alloys [2]. In view of the aforementioned problems, the current study investigated an approach which modified the SAC based solders with additives in order to improve the compliance without forming a large pasty range and sacrificing the creep resistance. The findings are presented and discussed below.

II. MATERIALS

The rigidity of SAC solders is mainly imparted by the Ag_3Sn and Cu_6Sn_5 intermetallic particles. To reduce the rigidity of high-silver containing SAC alloys, one potential approach is introducing additive elements which could remove those IMC particles. Based on the alloy phase diagram, Al reacts with both Ag and Cu, which promising a reduction in the quantity of Ag_3Sn and Cu_6Sn_5, is a very capable candidate. On the other hand, adding a small amount of Ni is reported to be beneficial, due to its effect in suppressing the growth of IMC scallop size and thickness on Cu [3]. Therefore, the work here studies the effect of addition of both Al and Ni onto SAC alloys, with emphasis on Al addition.

III. EXPERIMENTAL

Table 1 Tensile data for solder alloys.

	Yield strength (psi)	Tensile strength (psi)	Modulus (Ksi)	Elongation at break (%)
Sn94.49Ag3.99Cu0.64Ni0.88	5270 ± 248	7690 ± 470	2564 ± 677	11.8 ± 3.8
Sn94.43Ag3.97Cu0.64Al0.96	5521 ± 160	8530 ± 210	2369 ± 270	11.5 ± 4.2
Sn94.78Ag4.0Cu0.58Al0.6Ni0.04	3963 ± 436	6540 ± 920	2220 ± 332	14.3 ± 7.4
Sn94.92Ag4.23Cu0.33Al0.48Ni0.038	4587 ± 308	7510 ± 440	2163 ± 270	15.5 ± 6.4
Sn93.5Ag3.8Cu0.7Al0.05Ni2	5451 ± 236	7472 ± 220	2566 ± 317	12.3 ± 1.2
Sn96Ag3.6Cu0.13Al0.19	3965 ± 213	6434 ± 318	2671 ± 299	13.5 ± 4.4
Sn93.5Ag3.8cu0.7Al2Ni0.05	6146 ± 243	9470 ± 193	2923 ± 449	9.3 ± 1.1
Sn95.2Ag4Cu0.64Al0.19	4321 ± 325	6348 ± 449	2612 ± 298	17.0 ± 5.2
Sn97.3Ag1.65Cu0.5Al0.15Ni0.009	3919 ± 567	6620 ± 685	2466 ± 326	15.8 ± 5.2
Sn97.1Ag2.47Cu0.5Al0.196Ni0.012	3968 ± 292	7240 ± 298	2133 ± 487	21.2 ± 3.4
Sn96.7Ag2.9Cu0.5Al0.29Ni0.018	4032 ± 529	6534 ± 1120	2408 ± 331	16.0 ± 5.7
Sn95.3Ag3.92Cu0.62Al0.15Ni0.05	4175 ± 123	7178 ± 429	2357 ± 468	13.7 ± 5.4
Sn95.36Ag4Cu0.64Al0.073Ni0.0513	5461 ± 68	7580 ± 180	2668 ± 349	11.4 ± 2.0
Sn95.5Ag4Cu0.5	5971 ± 627	7470 ± 1070	2603 ± 471	17.3 ± 4.8
Sn95.5Ag3.8Cu0.7	6288 ± 411	8540 ± 770	2810 ± 322	16.4 ± 9.5
Sn96Ag3.5Cu0.5	5251 ± 324	7760 ± 760	2464 ± 210	17.3 ± 2.5
Sn96.5Ag3Cu0.5	5289 ± 707	7200 ± 1410	2412 ± 360	19.3 ± 6.7
Sn97Ag2.5Cu0.5	4887 ± 930	6050 ± 680	2194 ± 715	12.9 ± 1.5
Sn97.5Ag2Cu0.5	5113 ± 579	7050 ± 460	2316 ± 180	15.2 ± 7.9
Sn98Ag1.5Cu0.5	4317 ± 538	5970 ± 890	2239 ± 290	17.5 ± 5.8
Sn98.5Ag1Cu0.5	3359 ± 362	5640 ± 540	2152 ± 361	13.4 ± 4.3
Sn99Ag0.5Cu0.5	3438 ± 335	5900 ± 530	1921 ± 392	15.7 ± 6.0
Sn99.3Cu0.7	2768 ± 279	4260 ± 750	1666 ± 539	20.6 ± 8.8

Note: Ksi stands for thousand pounds per square inch.

Several tests were conducted on the new alloys, with SAC alloys as controls. The tests are described below.

1. Tensile Test

The sample alloy was cast into dumbbell shaped samples with water quenching process. The diameter and length of the cylinder central testing region is 0.125 inch and 2 inch, respectively. The sample was then tested with a MTS tensile tester. The crosshead speed used was 0.2 inch/min. The yield strength, ultimate tensile strength, elongation at break, and modulus were reported. 5-15 specimen were used for each alloy.

2. Microstructure

The dumbbell samples were also examined with both optical microscope and Scanning Electron Microscope for microstructure. In some incidences, EDX analysis was conducted on the sample for composition analysis.

3. Differential Scanning Calorimetry (DSC)

The sample alloy with a sample size about 5 mg was heated up to 260°C with scanning rate of 10°C/min, then cool down to -40°C at the same scanning rate. The heating and cooling procedure was repeated again. Data from the second heating run was used for alloy comparison.

4. Creep Test

Similar to tensile testing, a dumbbell shaped solder specimen was used for creep test. The stress range was explored for a measurable steady strain rate at room temperature. Two specimen were used for each combination of alloy and stress condition. The steady strain rate of at least two different stresses was determined for each alloy.

IV RESULTS

1. Tensile Test

The tensile data of the alloys tested are tabulated in **Table 1**.

The effect of alloy composition on yield strength is shown in **Fig. 1**. All SAC alloys contain around 0.5% Cu, therefore are denoted as SAC(n)05 where n stands for Ag content. Their values "SAC Yield Strength" are expressed as blue diamond data points, with trend line and equation given in the graph. All modified SAC alloys, SAC(n)05-XY, are denoted by the content of additions, such as Ni0.88. For SAC(n)05 system, the yield strength increases with increasing Ag content.

Conversely, addition of Al and Ni can result in a significantly reduced yield strength, particularly for the composition highlighted in the green shaded area in **Fig. 1**. Al appears to be the primary factor in reducing the yield strength. The dominant role of Al can be seen in **Fig. 2**, where the red bar data points are with Al addition only, and the diamond data points are with both Al and Ni additions. In all incidences, the amount of Ni is no more than 0.05%. Since both red and diamond data points fit

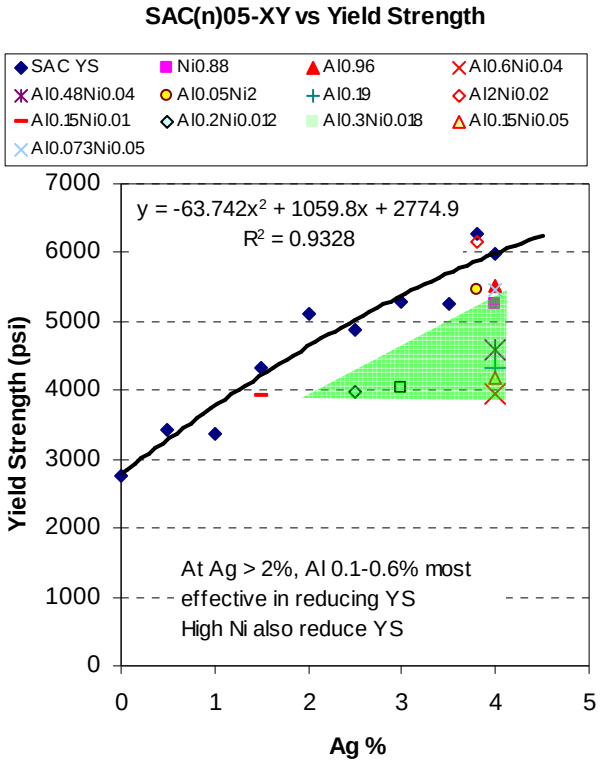

Fig. 1 Effect of alloy composition on yield strength.

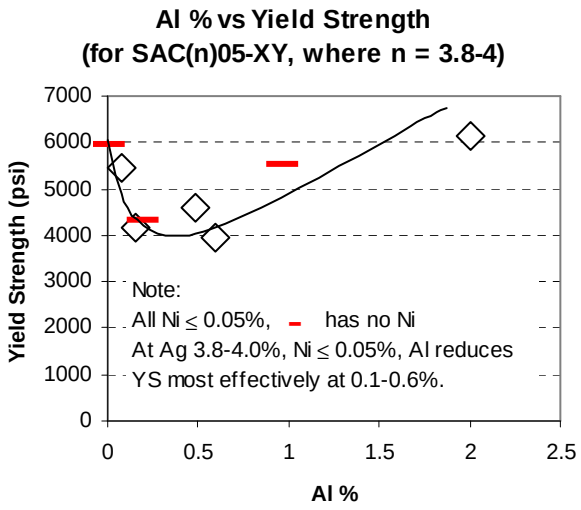

Fig. 2 Effect of Al addition on yield strength of SAC(n)05-XY

on the same trend curve, the effect of small amount of Ni is considered not very significant on yield strength. **Fig. 2** also indicates that at Ag 3.8-4.0% and Ni ≤ 0.05%, addition of Al 0.1-0.6% is most effective in reducing the yield strength. The lowest yield strength rendered by adding Al and Ni to SAC405 is about 4000 psi, which is about the same as that of SAC105 or SAC1505 (see **Fig. 1**).

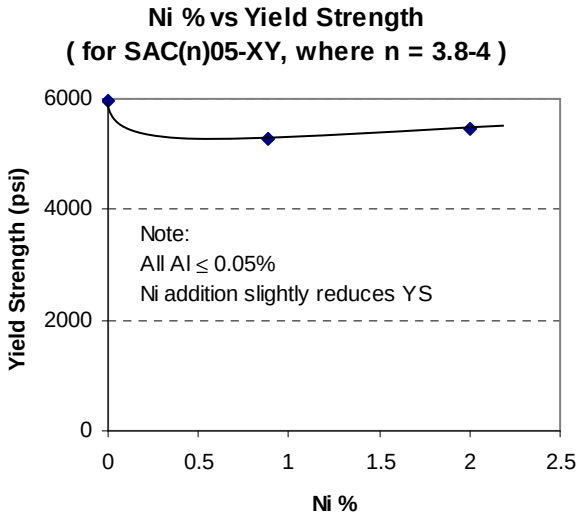

Fig. 3 Effect of Ni addition on yield strength of SAC(n)05-XY

Yet, at higher level of addition, the role of Ni on yield strength becomes quite more noticeable, as shown in **Fig. 3**. Here addition of Ni results in a slight decrease in yield strength. The extent of yield strength drop is about one-third of that of Al addition (see **Fig. 2**). This moderate effect on yield strength reduction may also be present at low Ni concentration, as suggested by **Fig. 3**.

For SAC(n)05 system, the tensile strength increases with increasing Ag content, as shown in **Fig. 4**. The effect of Al and Ni addition on tensile strength is not significant, as indicated by the data points of modified alloys scattered around the trend curve.

For SAC(n)05 system, while the data scattering is quite significant, the elongation at break appears to be insensitive to Ag content, as shown in **Fig. 5**. However, adding Al or Ni does cause a decrease in elongation at break, as highlighted by the dotted blue circle.

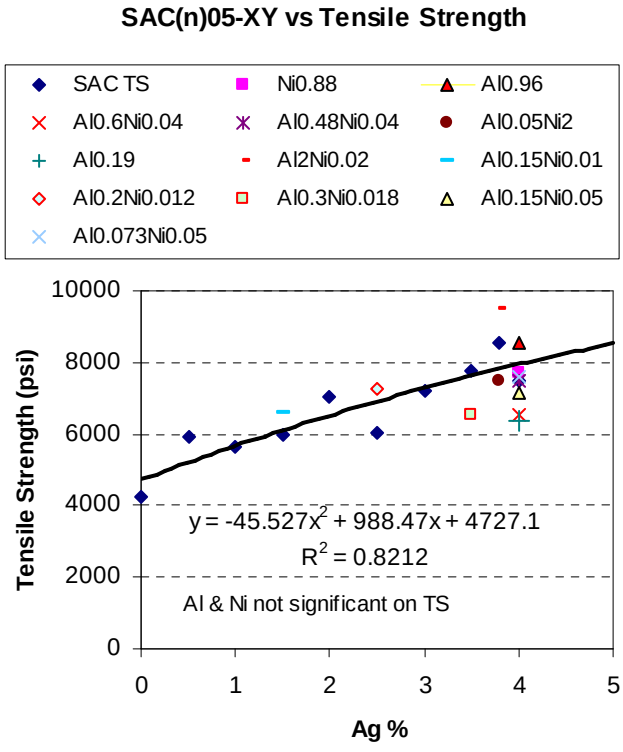

Fig. 4 Effect of alloy composition on tensile strength

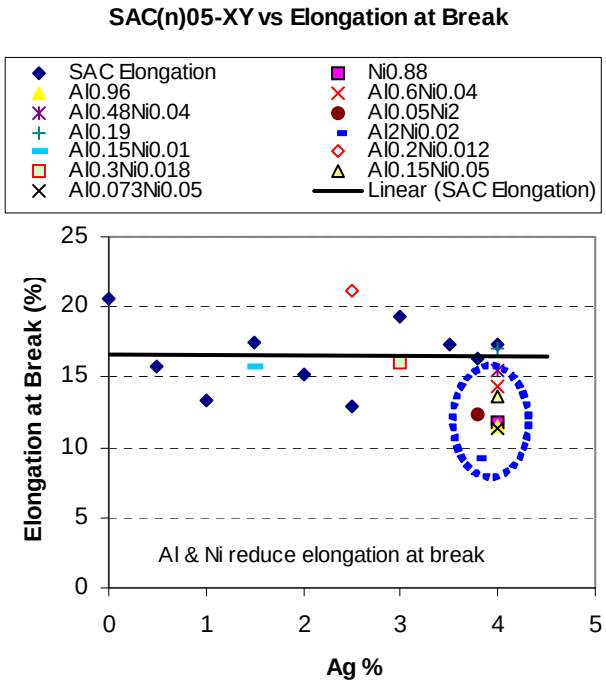

Fig. 5 Effect of alloy composition on elongation at break.

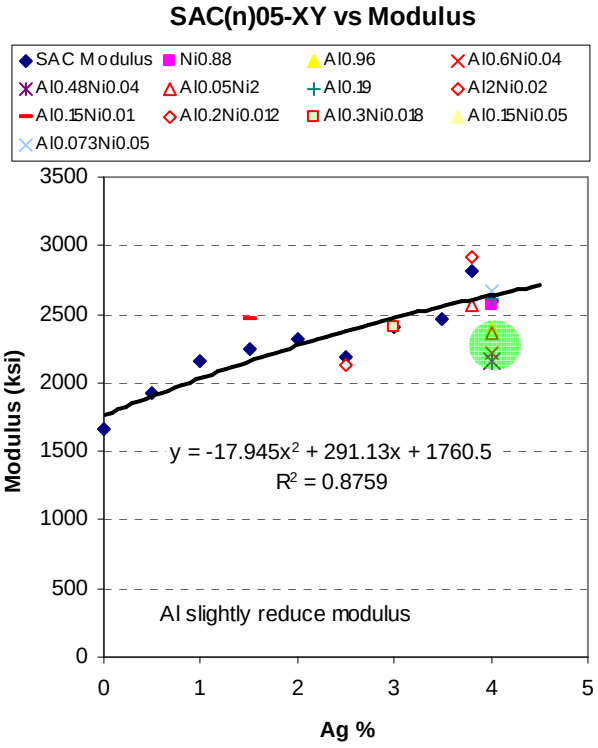

Fig. 6 Effect of alloy composition on modulus.

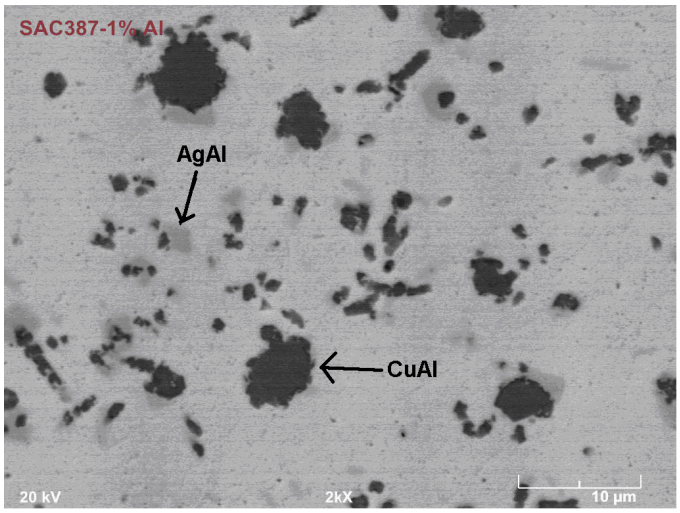

Fig. 7 SEM micrograph of Sn94.43Ag3.97Cu0.64Al0.96 (2000X).

For SAC(n)05 system, the modulus increases with increasing Ag content, as shown in **Fig. 6**. Addition of Al and Ni results in a slight decrease in modulus, as highlighted in the green zone.

2. Microstructure

The microstructure of SAC+Al, Sn94.43Ag3.97Cu0.64Al0.96, was examined with SEM, as shown in **Fig. 7**. Two distinct types of particles can be seen easily. The gray particle is Al8.2-Ag49.3-Sn42.2, and the dark particle is Al25.3-Cu71.3-Ag0.6-Sn2.8, as indicated in the EDX analysis results (see **Fig. 8)**. Presumably those particles are primarily IMC of AlAg and AlCu partially mixed with Sn. It is interesting to note that the weight ratio of Ag to Al is about 6:1, and the weight ratio of Cu to Al is about 3:1 here. Therefore, at Al content of 0.96%, most of the Ag and Cu in this alloy will be drained from the solder matrix and be associated with Al.

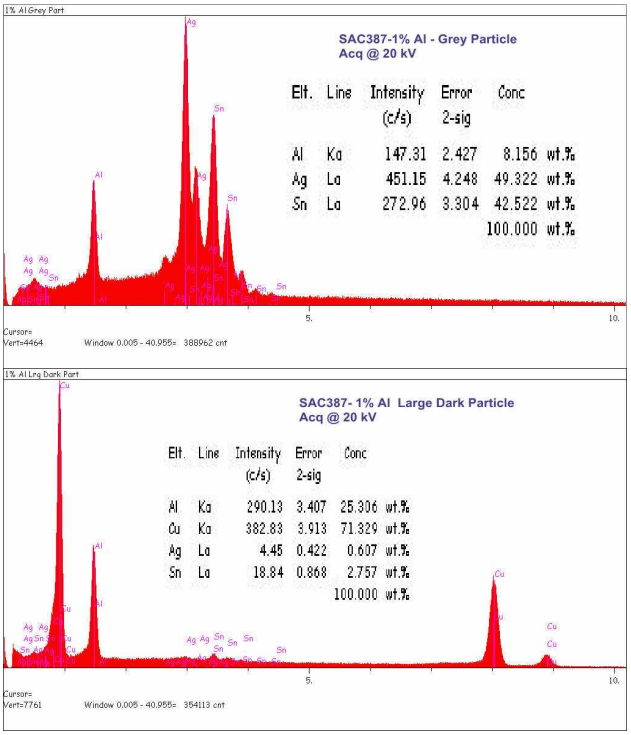

Fig. 8 EDX graph on gray (top) and dark (bottom) IMC particles of Sn94.43Ag3.97Cu0.64Al0.96.

Fig. 9 shows SEM 200X picture of SAC+Ni, Sn94.49Ag3.99Cu0.64Ni0.88. Many long gray needles are observed in the solder, with a length of

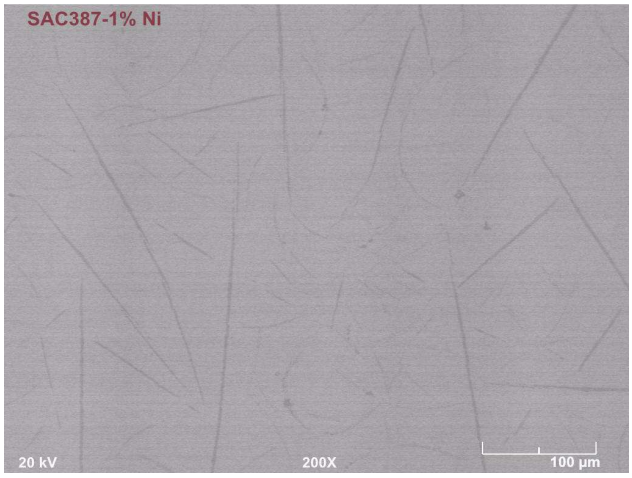

Fig. 9 SEM micrograph of Sn94.49Ag3.99Cu0.64Ni0.88 (200X).

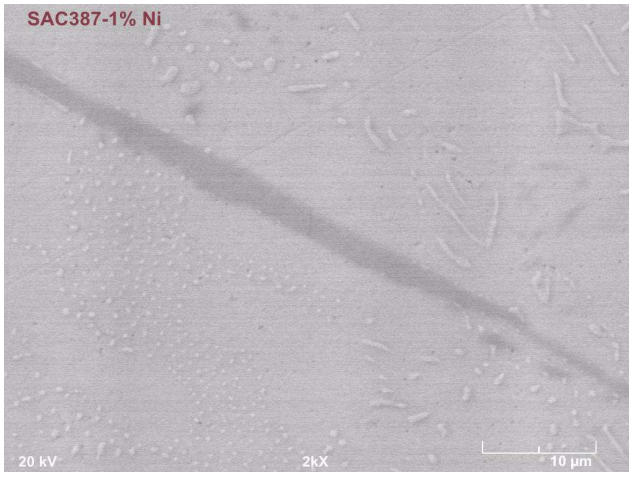

Fig. 10 SEM micrograph of Sn94.49Ag3.99Cu0.64Ni0.88 (2000X).

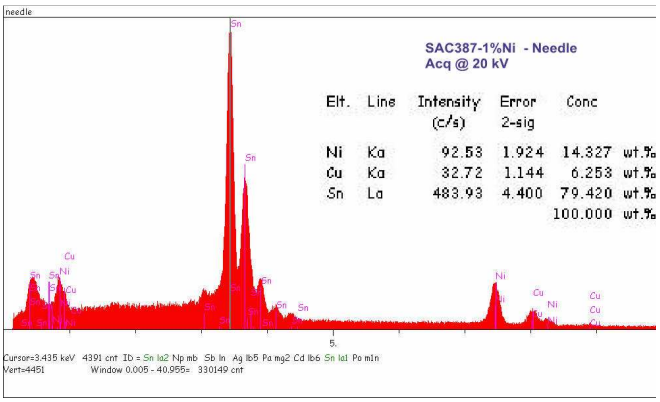

Fig. 11 EDX graph on gray needle shown in Sn94.49Ag3.99Cu0.64Ni0.88.

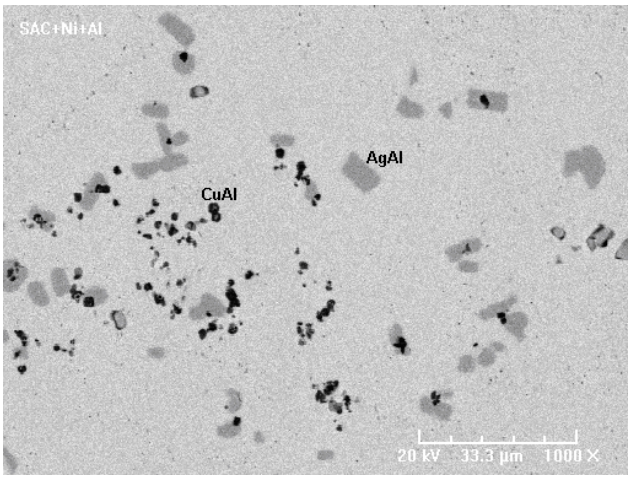

Fig. 12 SEM micrograph of Sn94.78Ag4.0Cu0.58Al0.6Ni0.04 (1000X).

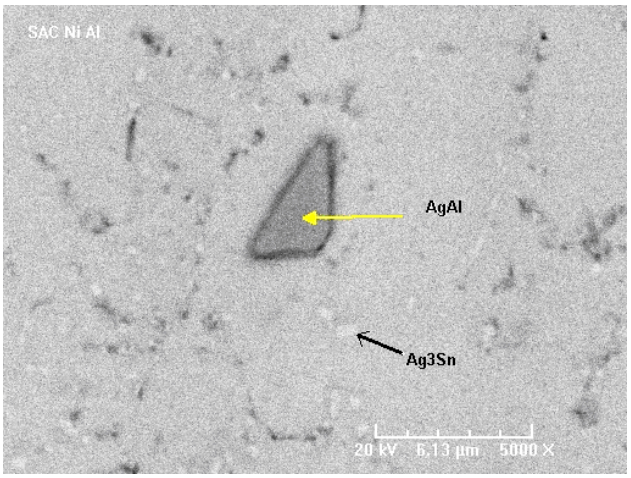

Fig. 13 SEM micrograph of Sn94.78Ag4.0Cu0.58Al0.6Ni0.04 (5000X).

several hundred microns. A close-up picture (see

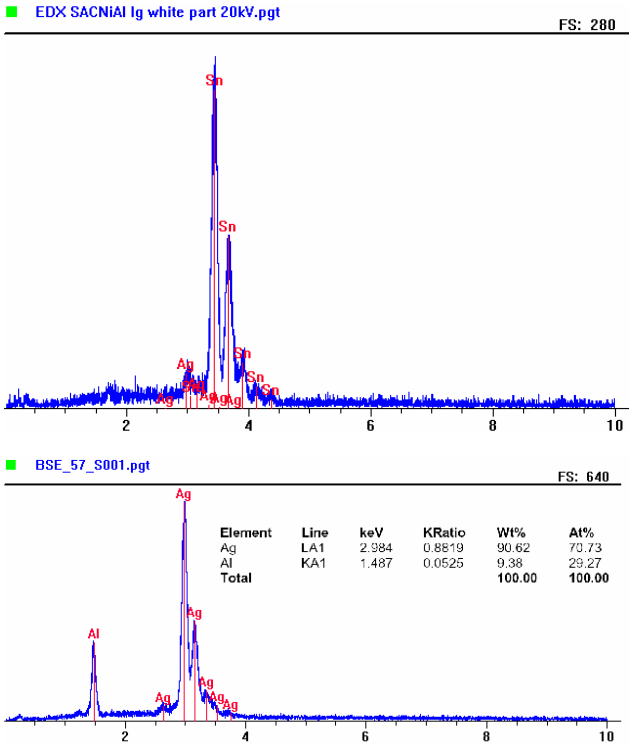

Fig. 14 EDX graphs of bright particle (top) and gray particle (bottom) shown in Fig. 13.

Fig. 10) displays many bright Ag_3Sn IMC particles in the form of micron-sized round particles or short rods. The gray needle was identified via EDX as Ni14.3-Cu6.3-Sn79.4, presumably mainly $(Ni,Cu)_3Sn_4$, as shown in **Fig. 11**. The weight ratio of Ni to Cu is about 2.3:1. With Ni concentration being 0.88%, the Cu entrapped in the $(Ni,Cu)_3Sn_4$ is estimated to be about 0.4%. In other words, Cu will be highly depleted by Ni-Cu-Sn IMC formation. As a result, the SAC matrix composition here is expected to be greatly skewed toward near-eutectic Sn-Ag structure. The DSC data to be presented in the next section strongly supports this speculation.

SAC+Al+Ni, Sn94.78Ag4.0Cu0.58Al0.6Ni0.04, was also examined with SEM, as shown in **Fig. 12**. Many large gray particles and small dark particles are observed. A close-up look at area near the gray particle (see **Fig. 13**) shows many tiny bright particles around the gray particle. The bright particles are speculated to be Ag_3Sn IMC, although the Ag content is lower than expected, as shown in the top graph of **Fig. 14**. The large gray particle is Al9.4-Ag90.6, as indicated by the EDX data shown in bottom graph of **Fig. 14**. Here the weight ratio of

Al to Ag is approximately 1:10, indicating the extraordinary ability of Al to drain Ag from SAC matrix. The dark small particle, as shown in **Fig. 15**, is Al32.2-Cu57.1-Sn10.7 (see **Fig. 16**). The findings here are in line with what was observed in the SAC+Al alloy discussed previously.

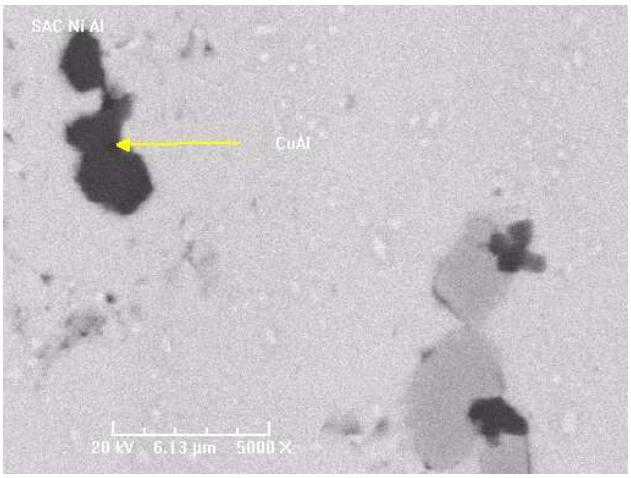

Fig. 15 SEM micrograph of Sn94.78Ag4.0Cu0.58Al0.6Ni0.04 (5000X).

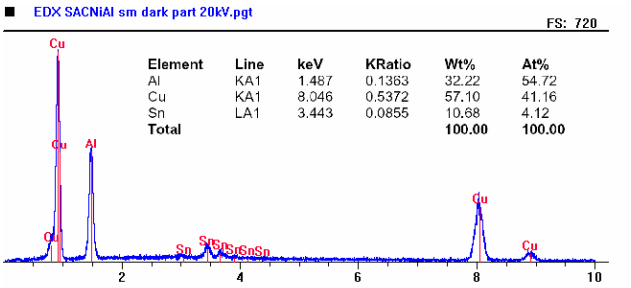

Fig. 16 EDX graph of dark particle shown in Fig. 15.

3. DSC

The DSC heating curves of SAC387, SAC+Al (Sn94.43Ag3.97Cu0.64Al0.96), and SAC+Ni (Sn94.49Ag3.99Cu0.64Ni0.88) are shown in **Fig. 17**. SAC387 shows an onset temperature at 218.6°C and a peak temperature (liquidus) at 219.2°C.

Two endotherm peaks are observed for SAC+Al, with the primary peak (liquidus) at 225.9°C, the secondary peak at 221.2°C, and the onset temperature at 220.4°C. In the microstructure section, it was concluded that most of the Ag and Cu in this SAC+Al alloy should be drained from the solder matrix and be associated with Al. As a result, for this SAC-based alloy, instead of forming near-ternary-eutectic SAC composition, it very likely forms near-SnAg eutectic and near-Sn-Cu eutectic structures, as suggested by the two peaks observed in DSC heating thermograph. Also co-exist in the system should be AlAg and AlCu IMC particles.

For SAC+Ni, Sn94.49Ag3.99Cu0.64Ni0.88, the onset temperature and the peak temperature are 219°C and 220.4°C, respectively. As discussed earlier, Cu is virtually depleted from the matrix due to the formation of $(Ni,Cu)_3Sn_4$. Consequently the copper-striped matrix becomes near-eutectic SnAg structure. Indeed, this is supported by the DSC data, where the peak temperature is close to the melting temperature 221°C of eutectic Sn-Ag, as shown in **Fig. 17**.

SAC405 and SAC405+Al(Ni) alloys, including Sn95.2Ag4Cu0.64Al0.19, Sn94.78Ag4.0Cu0.58Al0.6Ni0.04, and Sn94.43Ag3.97Cu0.64Al0.96, are shown in **Fig. 18**. With increasing Al content, the DSC endotherm curve gradually shifts from lower to higher peak temperatures, and from single to dual peaks. Thus, at 0% Al (SAC405), the peak temperature is 219.5°C. At 0.19% Al (Sn95.2Ag4Cu0.64Al0.19), the peak temperature is 221.2°C. At 0.6% Al (Sn94.78Ag4.0Cu0.58Al0.6Ni0.04), the peak is about to split, with higher temperature shoulder being 222.2°C. At 0.96% Al (Sn94.43Ag3.97Cu0.64Al0.96), the endotherm splits into two peaks, with the higher peak (liquidus) temperature being 225.9°C.

As discussed above, increase in Al content will drain more Ag and Cu from the SAC system. This in turn causes a shift of SAC405 from near ternary eutectic composition towards combination of eutectic SnAg and eutectic SnCu. At Al content greater than 0.6%, the liquidus temperature increases more rapidly with continued increase in Al content, as shown in **Fig. 19**.

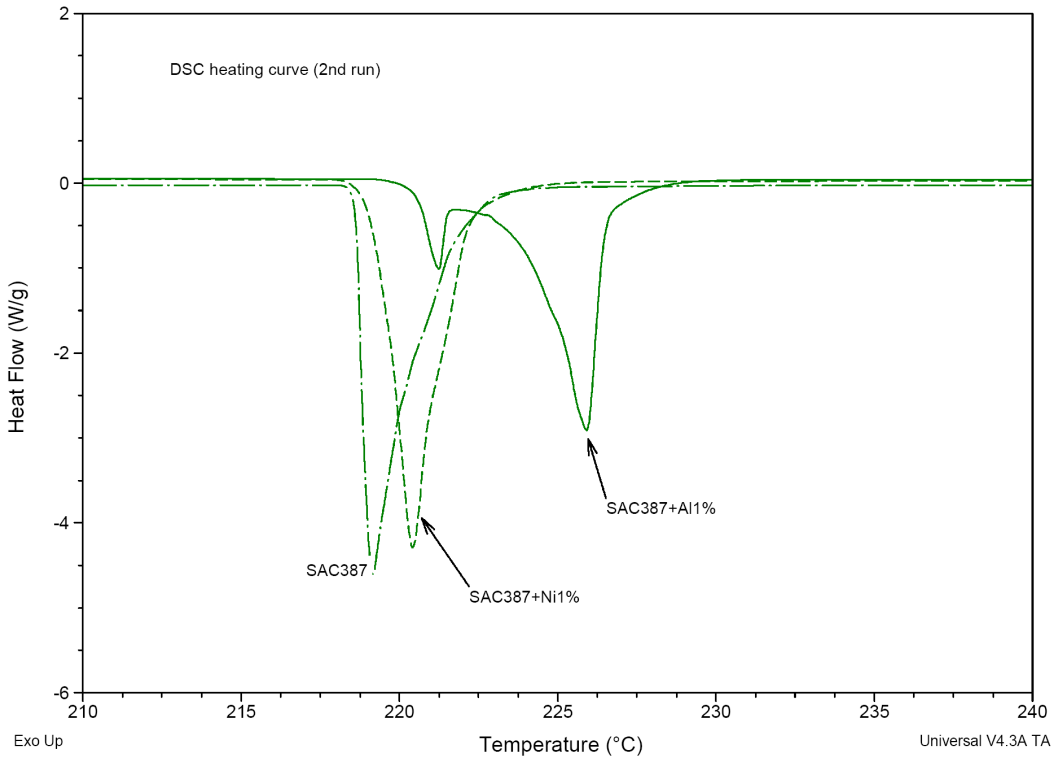

Fig. 17 DSC thermographs (second run heating) of SAC387, SAC+Al (Sn94.43Ag3.97Cu0.64Al0.96), and SAC+Ni (Sn94.49Ag3.99Cu0.64Ni0.88).

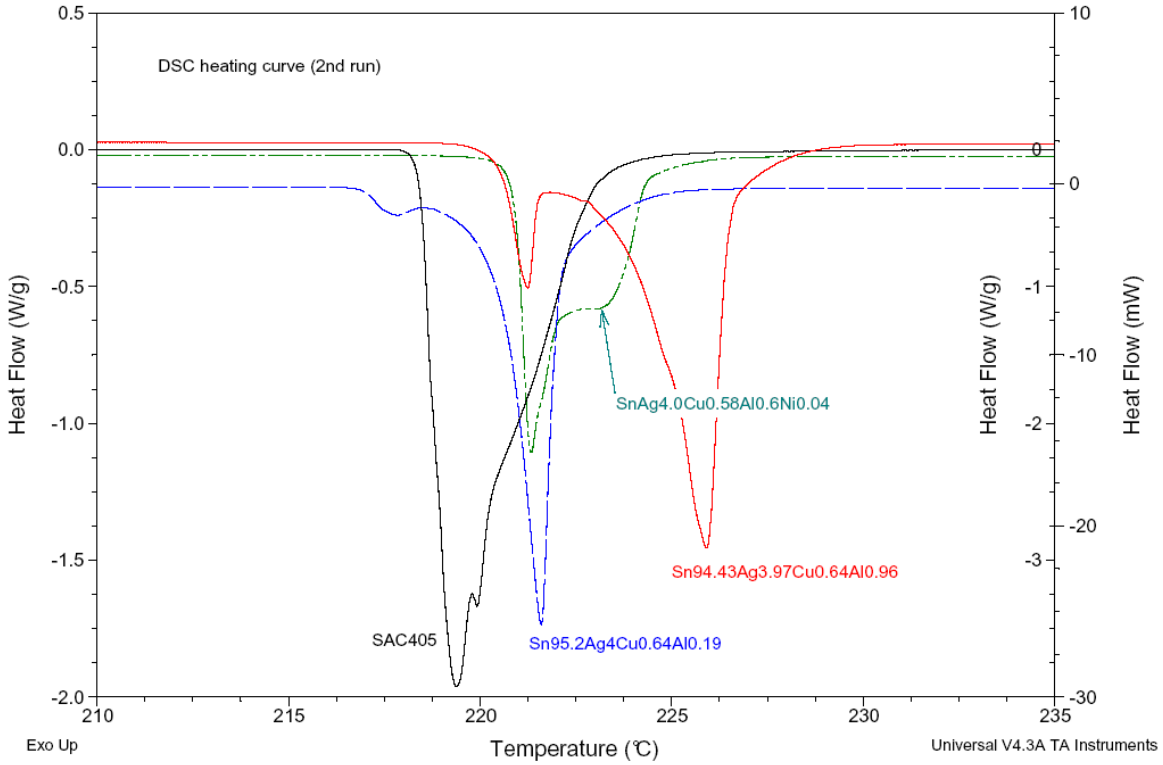

Fig. 18 DSC thermographs (second run heating) of SAC405 and SAC405+Al(Ni) alloys, including Sn95.2Ag4Cu0.64Al0.19, Sn94.78Ag4.0Cu0.58Al0.6Ni0.04, and Sn94.43Ag3.97Cu0.64Al0.96.

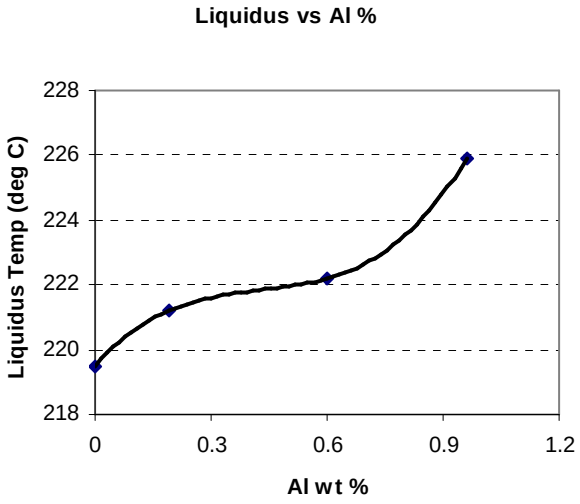

Fig. 19 Liquidus temperature of SAC+Al(Ni) alloys as a function of Al content.

Compared with SAC105 and SAC1505, the SAC405+Al+Ni alloys exhibit both a lower liquidus temperature and a narrower pasty range. **Fig. 20** shows DSC thermographs of SAC105, SAC1505, Sn95.3Ag3.92Cu0.62Al0.15Ni0.05, and Sn94.78Ag4.0Cu0.58Al0.6Ni0.04. The two modified alloys are about 4°C lower in both liquidus temperature and pasty range than that of SAC105 and SAC1505.

4. Creep Test

The creep test data of modified alloys are exemplified by SAC405+Al+Ni, namely Sn95.3Ag3.92Cu0.62Al0.15Ni0.05 and Sn94.78Ag4.0Cu0.58Al0.6Ni0.04. The yield strength of both alloys is much lower than SAC405, and is between that of SAC105 and SAC1505, as shown in **Table 1**. The creep rate data of SAC105, SAC1505, SAC305, and SAC405 are also shown for comparison purposes, as indicated in **Fig. 21**. Within the stress range studied, both modified alloys exhibit a steady creep rate lower than that of SAC105 and SAC1505, roughly comparable with that of SAC305, and are higher than SAC405. The comparison with SAC305 and SAC405 is based on estimation using extrapolation.

The creep data suggests that, although Al and Ni doping causes SAC405 to be softened to the level of SAC105 and SAC1505, the potential fatigue

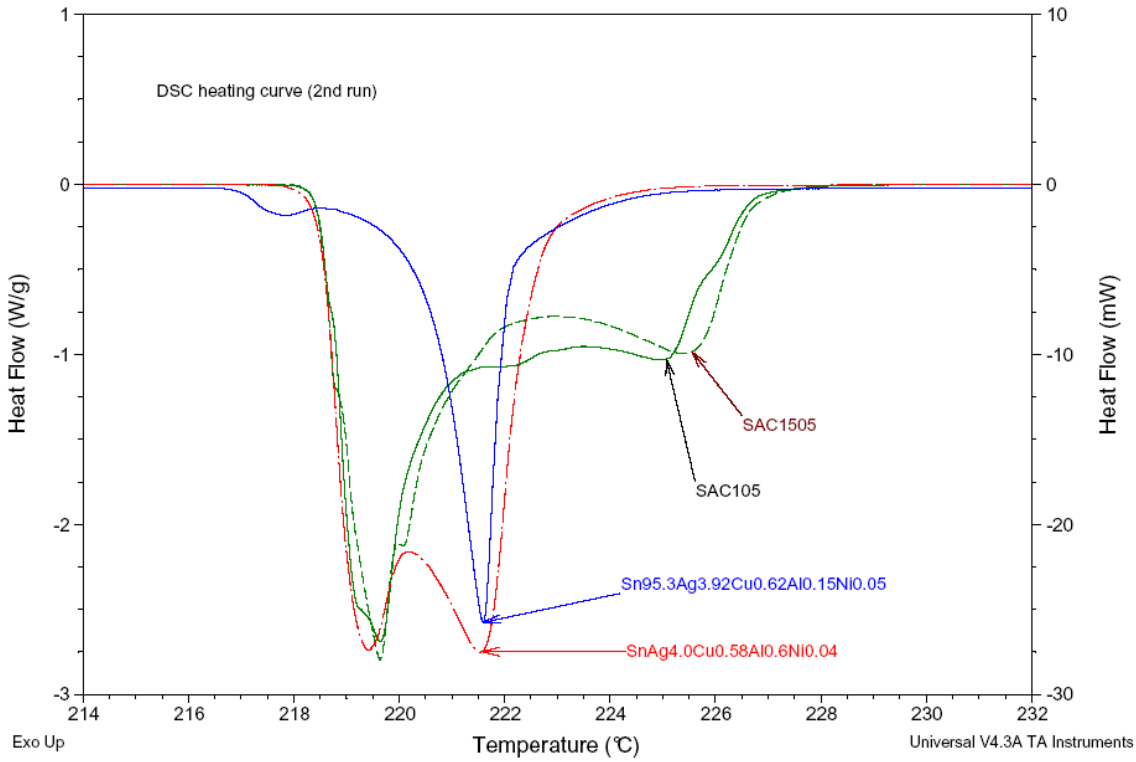

Fig. 20 DSC thermographs (second run heating) of SAC105, SAC1505, and SAC405+Al+Ni alloys, including Sn95.3Ag3.92Cu0.62Al0.15Ni0.05 and Sn94.78Ag4.0Cu0.58Al0.6Ni0.04.

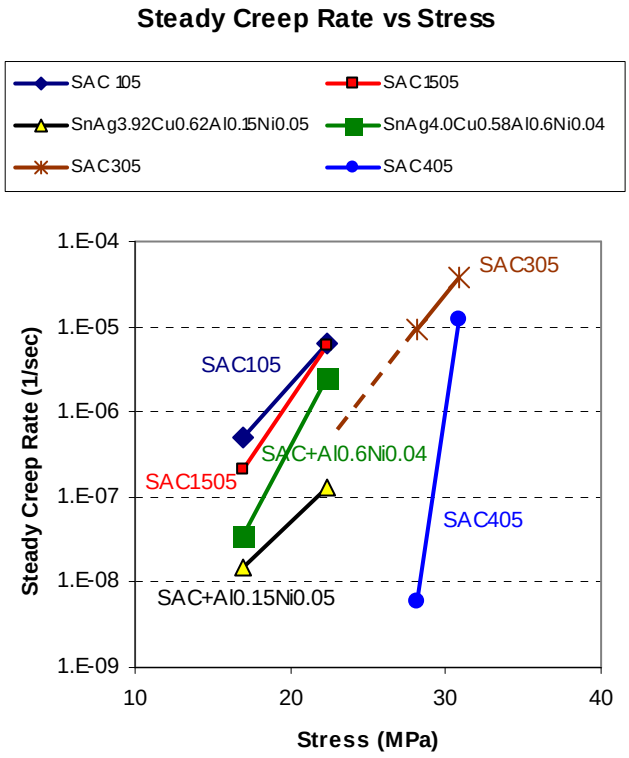

Fig. 21 Effect of alloy on steady creep rate.

behavior of doped SAC405 is maintained at the level of SAC305.

V. DISCUSSION

1. Softening

The yield strength reduction is mainly attributed to the reduction in number of small, hard Ag_3Sn IMC particles due to formation of large non-stoichiometric AlAg IMC particles. The remaining number of Ag_3Sn particles may have been reduced to the level of SAC105 or SAC1505. Reduction in Cu_6Sn_5 particles due to formation of non-stoichiometric AlCu and large $(Ni,Cu)_3Sn_4$ IMC particles should also contribute to this phenomenon. The non-stoichiometric IMC particles are expected to be softer than the hard stoichiometric Ag_3Sn particles. Furthermore, a smaller number of large particles is less effective in strengthening than a larger number of small particles.

2. Creep Rate

Non-stoichiometric IMC particle or large particle, although less effective in increasing yield strength, are considered still harder than Sn, therefore they are expected to provide resistance in creep.

VI. CONCLUSION

Addition of Al into SAC alloys reduces the number of hard Ag_3Sn and Cu_6Sn_5 IMC particles, and forms larger, softer non-stoichiometric AlAg and AlCu particles. This results in a significant reduction in yield strength, and also causes some moderate increase in creep rate. For high Ag SAC alloys, adding Al 0.1-0.6% to SAC alloys is most effective in softening, and brings the yield strength down to the level of SAC105 and SAC1505, while the creep rate is still maintained at SAC305 level. Addition of Ni results in formation of large $(Ni,Cu)_3Sn_4$ IMC particles and loss of Cu_6Sn_5 particles. This also causes softening of SAC alloys, although to a less extent than that of Al addition. Addition of Al also drives the microstructure to shift from near-ternary SnAgCu eutectic toward combination of eutectic SnAg and eutectic SnCu. Addition of Ni drives a shift toward eutectic SnAg. For SAC+Al+Ni alloys, the pasty range and liquidus temperature are about 4°C less than that of SAC105 or SAC1505 if the added quantity is less than about 0.6%. Addition of Al and Ni also results in a slight decrease in modulus and elongation at break, although the tensile strength is not affected.

VII. REFERENCE

1. Yoshiharu Kariya, Takuya Hosoi, Shinichi Terashima, Masamoto Tanaka, Masahisa Otsuka, “Effect of silver content on the shear fatigue properties of Sn-Ag-Cu flip-chip interconnects”, Journal of electronic materials , vol. 33, no. 4, 2004, p. 321- 328
2. S. K. Kang, P. A. Lauro, D. Y. Shih, D. W. Henderson, and K. J. Puttlitz, “Microstructure and mechanical properties of lead-free solders and solder joints used in microelectronic applications”, IBM Journal of Research ad Development, on-line publication: http:/researchweb.watson.ibm.com/journal/rd/494/kang.html
3. Masazumi Amagai (Texas Instruments, Japan), " A Study of Nano Particles in SnAg-Based Lead Free Solders for Intermetallic Compounds and Drop Test Performance", 56th ECTC Proceedings, P. 1170-1190, San Diego, CA, May 30-June 2, 2006